PROCEEDINGS, 45th Workshop on Geothermal Reservoir Engineering
Stanford University, Stanford, California, February 10-12, 2020
SGP-TR-

Predicting thermal responses at the EGS Collab testbed based on tracer test-inferred flow fields

Hui Wu, Pengcheng Fu, Joseph P. Morris

Atmospheric, Earth, and Energy Division, Lawrence Livermore National Laboratory, Livermore, CA 94550

E-mail address: wu40@llnl.gov

Keywords: enhanced geothermal systems, EGS Collab, thermal response, tracer modeling, thermal modeling

ABSTRACT

The EGS Collab project is an ongoing *in situ* experiment designed to investigate the stimulation of fractures in rock and the circulation of fluids in the stimulated fracture network for enhanced geothermal system (EGS) applications. Following multiple hydraulic stimulations, a series of tracer tests were performed to understand flow characteristics between injection and production wells, and a long-term chilled-water circulation test was conducted to investigate the thermal behavior in the system. The present study aims to predict the thermal responses at the production well using flow fields characterized by tracer tests. We first apply a stochastic approach to performing massive realizations to simulate tracer transport processes in the stimulated hydraulic fracture. From the realizations that successfully reproduce the field tracer data, we retrieve the flow field in the fracture which is further used in subsequent thermal modeling to analyze heat transport behavior in the EGS Collab testbed. The simulated thermal responses at the production well are demonstrated, and the thermal breakthrough time is predicted from the modeling results.

1. INTRODUCTION

Enhanced geothermal system (EGS) is a technique that tries to extract heat resources stored in subsurface hot dry rocks (HDR). Due to the generally low permeability of HDR, engineering measures such as hydraulic fracturing and shearing are employed to stimulate new fractures in the target HDR to promote fluid flow and enlarge effective heat exchange area. Fluid is then circulated in the stimulated fracture network to extract heat energy. The performance of an EGS highly depends on the flow characteristics in the stimulated fracture network (Brown et al., 2012; Fu et al., 2016; Guo et al., 2016; Hawkins et al., 2018). Tracer testing is a powerful diagnostic tool for hydraulic connectivity characterization in subsurface reservoirs, and has been widely used in many EGS sites such as the Fenton Hill EGS site in New Mexico, the Soultz-sous-Forêts EGS site in France, the Habanero EGS site in Australia, and so on (Rodrigues et al., 1993; Brown et al., 2012; Radilla et al., 2012; Vogt et al., 2012; Ayling et al., 2016). Efforts have been devoted to predicting thermal responses from tracer testing results. For example, Shook (2001) applied analytical solutions to transform tracer history to temperature history. Wu et al. (2008) developed a semi-analytical approach to calculating enthalpy production from fractured geothermal reservoirs using partitioning tracer results. Guo et al. (2016) investigated the relationship between tracer test indices (peak concentration and mean residence time) and the lifetime of a single-fracture EGS. Hawkins et al. (2018) discussed the use of different tracers (adsorptive and inert tracers) for thermal breakthrough predictions. Many progresses have been achieved using either synthetic data or field measurements. However, due to the many uncertainties pertaining to subsurface EGS reservoirs, the interpretation of field tracer data for thermal response predictions still remains a challenge.

The EGS Collab project is a field experiment aiming to provide a means of testing models, tools, and concepts that can be applied for successful EGS reservoir development. The project is planned to have three phases of experiments, and the Experiment 1 testbed is located in a predominately phyllite rock, approximately 1478 m below ground surface, on the western side of the West Access Drift within the Sanford Underground Research Facility (SURF) in South Dakota, USA. From May 2018, the project has been performing both stimulation and flow characterization experiments in the Experiment 1 testbed (Kneafsey et al., 2019; White et al., 2019). A long-term chilled-water circulation test started on May 8, 2019 and continues to current. Various data were collected to characterize the stimulated fracture network and understand the thermal behavior in the testbed, including ERT data, seismic events, distributed temperature sensing data, as well as a series of tracer data.

The main objective of this study is to analyze the thermal processes in the EGS Collab Experiment 1 testbed during the chilled-water circulation test and predict thermal responses using flow fields interpreted from tracer data. A high-fidelity fracture network model developed from geological and geophysical observations and measurements was utilized to perform tracer simulation through a stochastic approach. A 3D model containing both the fracture network model and rock formation surrounding the fracture network was then developed for subsequent thermal modeling.

2. EXPERIMENT 1 OF THE EGS COLLAB PROJECT

Fig. 1(a) shows the well configuration in the Experiment 1 testbed of the EGS Collab project. Eight wells were drilled from the drift wall into the testbed, including an injection well (E1-I) which is nominally in the direction of the minimum horizontal principal stress, a production well (E1-P) parallel to E1-I and approximately 10 m to the east of E1-I, four monitoring wells (E1-PDT, E1-PDB, E1-PST and E1-PSB) parallel to the expected hydraulic fracture plane, and two monitoring wells (E1-OT and E1-OB) largely orthogonal to the expected hydraulic fracture. In Experiment 1, several stimulation activities were performed between May and December 2018 at different depths (39.0 m, 43.3 m, and 50.0 m) along E1-I to create hydraulic fractures to connect E1-I and E1-P (Fig. 1(a)). Following the stimulation at the 50 m depth, a series of water circulation and tracer tests were conducted at the same depth. On May 8 2019, a chilled-water

circulation test started with the injection temperature at 11.5 °C and the injection rate 400 ml/min. The details of the stimulation activities as well as the water circulation and tracer tests are described in White and Fu (2020).

In this study, we focus on the fracture network stimulated at the 50 m depth since most of the following water circulation and tracer tests were performed at this depth. A conservative tracer test during the chilled-water circulation test (conducted on July 24, 2019) is selected to analyze the flow characteristics in the fracture network. In this tracer test, 2.8 g C-Dots (a nanoparticle tracer consisting of a carbon core decorated with a highly fluorescent polymer) were injected into the system with an initial concentration of C_0 = 1297 ppm. Fig. 2 shows the measured tracer breakthrough curves (BTCs). Although water flowed out of the system from E1-P, E1-OT, E1-PDT and E1-PST (as listed in Fig. 2), C-Dots were only detected at E1-P, E1-OT and E1-PDT. Note that water and tracer flowed out of E1-P from two locations separated from each other through a packer system. One is the location at approximately 39.5 m deep and the other location is approximately 2.2 m shallower. We denote the two locations as E1-PHF and E1-PNF (HF=hydraulic fracture(s), NF=natural fracture(s), as will be explained in section 3.1) respectively).

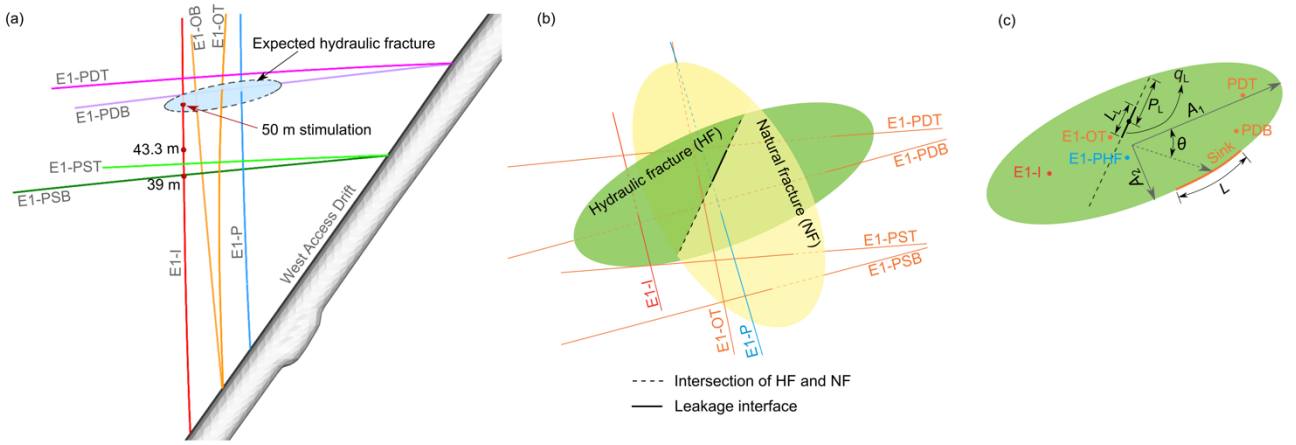

Figure 1: Well configuration of the Experiment 1 of the EGS Collab project and the developed fracture network model for tracer modeling. (a) Configuration of injection, production and monitoring wells. The stimulation depths are annotated. An expected hydraulic fracture is also shown. (b) Fracture network model. (c) Parameters in the hydraulic fracture.

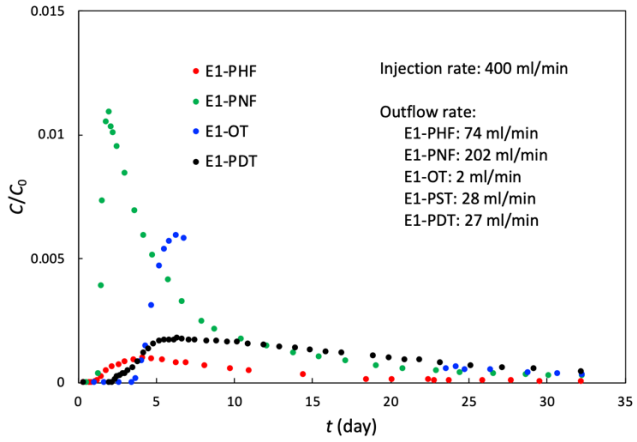

Figure 2: Tracer breakthrough curves from the C-Dots tracer test on July 24, 2019. The injection rate as well as the outflow rates from different wells are annotated.

3. MODEL AND METHODOLOGY

3.1 Tracer modeling

Based on the geological and geophysical measurements (core logs, wellbore images, microseismic events, DTS signals, and a camera survey in E1-P), Wu et al. (2019) developed a fracture network model for the EGS Collab Experiment 1 testbed, which is also used for tracer modeling in this study. The fracture network model involves an elliptical hydraulic fracture and an elliptical natural fracture (Fig. 1(b)), and the two fractures are coupled by treating a segment of the intersection line between the two fractures as the connection (i.e. a leakage interface) between them. Fluid carrying tracer flows from the hydraulic fracture to the natural fracture through this leakage interface. E1-PHF and E1-PNF are the intersections between E1-P and the hydraulic and natural fractures respectively.

In this study, we focus on the thermal behavior in the hydraulic fracture, and therefore the tracer modeling is only performed for the hydraulic fracture to reproduce the tracer breakthrough curves at E1-OT and E1-PHF (Fig. 2). Parameters for the hydraulic fracture include

the two semi-axis lengths A_1 and A_2, aperture w, hydrodynamic dispersion coefficient D_f, and three parameters representing the leakage interface (P_L and L_L for the location and length of the leakage interface, and q_L for the leakage rate). Since the fluid and tracer were not fully recovered in the tracer test, we assume a sink on the periphery of the hydraulic fracture to account for fluid/tracer leakage to natural fractures that are not explicitly included in the model (Fig. 1(c)). Two parameters θ and L are used to describe the location and length of the sink respectively. We consider both a uniform aperture scenario and a spatially-autocorrelated heterogeneous aperture scenario. For the uniform aperture scenario, the aperture distribution is described by a single parameter (w), whereas for the heterogeneous aperture scenario, the aperture distribution is described by three parameters, including average aperture ($\overline{w}$), standard deviation (σ) and correlation length (CL). The ranges of these parameters can be found in Wu et al. (2019).

We use the stochastic approach developed in Wu et al. (2019) to model the tracer transport process in the hydraulic fracture. For each tracer simulation, the injection and outflow rates in Fig. 2 are used as boundary conditions. Except for the sink, the boundaries along the perimeters of the hydraulic fracture are assumed to be impermeable to both fluid and tracer. Note that the matrix is not considered in the tracer simulation.

3.2 Thermal modeling

To model the chilled-water circulation test, we developed a 3D thermal model based on the fracture network model in Fig. 1(b). The 3D thermal model includes the hydraulic and natural fractures as well as the rock formation surrounding the fractures. The dimensions of the 3D thermal model are approximately 120 × 100 × 90 m, and the two fractures are represented by two thin layers 0.004 m in thickness. The injection well (E1-I) is represented by a column layer with a cross section size of 0.1 × 0.1 m. The mesh resolution near E1-I and the two fractures is 0.1 m, and gradually increases to 2 m in the far field. The computational domain consists of approximately 1,685,000 elements.

White et al. (2018) developed a 2D computational domain to model the temperature, pore pressure and fluid saturation profiles around the West Access Drift at SURF. The ambient geothermal gradient, hydrological state and historical miming operations (excavation, flooding, dewatering, and mine closure) were considered in the model and the modeling results were validated against temperature measurements taken during the EGS Collab project within the kISMET boreholes (Oldenburg et al., 2016; Roggenthen and King, 2017). The obtained temperature profiles are used as initial temperature conditions in our thermal modeling. As shown in Fig. 3(a), the initial temperature is the smallest near the drift and increases in a radial pattern around the drift since the system is generally dominated by radial heat transport and fluid flow. The initial temperature difference between the injection point and E1-PHF is approximately 0.8 °C.

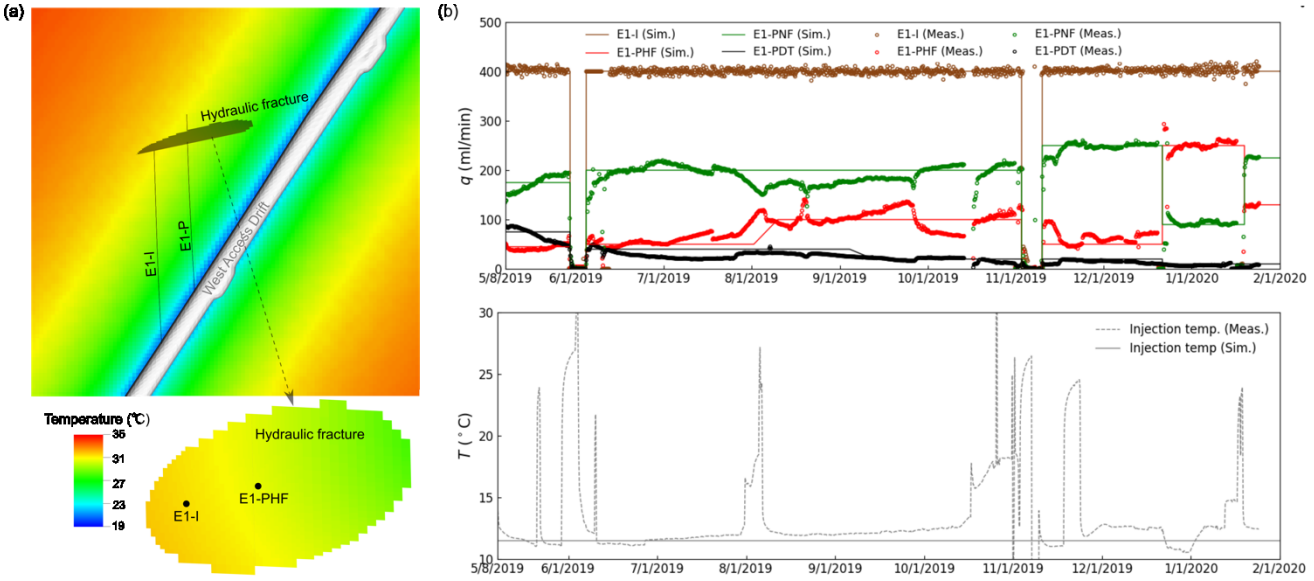

Figure 3: Initial temperature profile in the model and flow/temperature measurements during the chilled-water circulation test. (a) Initial temperature distribution around the drift. Temperature distribution in an assumed hydraulic fracture is also shown. (b) Injection and outflow rates as well as injection temperature. The solid lines are field measurements and the dash lines are fitted step functions used in the thermal simulations.

During the chilled-water circulation test, the injection rate remained almost at 400 ml/min (except several shut-in periods as shown in Fig. 3(b)), while the measured outflow rates from E1-PHF, E1-PNF and E1-PDT varied drastically. In the thermal modeling, we use step functions to approximate the outflow rate changes (Fig. 3(b)). The outflow at E1-OT is only about 2 ml/min and is ignored in the thermal modeling. The outflow rate at E1-PST is not considered since E1-PST does not intersect the hydraulic fracture. The sink obtained from tracer modeling is used as a pressure boundary. The effect of chilled-water injection includes two aspects: (1) Part of E1-I that connects the drift and the hydraulic fracture (Fig. 3(a)) behaves like a constant low temperature segment and affects the temperature response at the production well through thermal conduction. (2) The flow of chilled water within the hydraulic fracture affects the temperature response at the production well mainly through thermal convection. Both of the two aspects are considered in the thermal modeling. The

parameters for rock and fluid properties used in the thermal modeling are listed in Table 1. According to previous studies (Fu et al., 2018; White et al., 2018), a rock thermal conductivity of 5 W/m/K is adopted.

Table 1: Rock and water parameters used for thermal modeling.

Parameter	Value	Parameter	Value
Porosity of rock	0.003	Permeability of rock (m^2)	2×10^{-18}
Solid density of rock (kg/m^3)	2500	Specific heat capacity of rock (J/kg/K)	790
Specific heat capacity of water (J/kg/K)	4460	Water viscosity (Pa·s)	0.001
Water compressibility (Pa^{-1})	2×10^{-10}	Thermal conductivity of rock (W/m/K)	5

4. RESULTS AND DISCUSSIONS

4.1 Reproduction of tracer BTCs

With the stochastic tracer modeling approach in Wu et al. (2019), approximately 150,000 realizations were performed under the uniform aperture scenario and 140,000 realizations under the heterogeneous aperture scenario. Under the uniform aperture scenario, we select the realization that yields the best fit of the BTCs at E1-PHF and E1-OT for subsequent thermal modeling. The comparison of the measured and simulated tracer BTCs are shown in Fig. 4 (a). Under the heterogeneous aperture scenario, three realizations that match the measured tracer BTCs almost equally well are selected for subsequent thermal modeling (Fig. 4(b)). The corresponding aperture fields are also shown. Although the four aperture fields in Fig. 4 are different, all of them can reproduce the measured tracer BTCs at E1-PHF and E1-OT. A commonality among them is that the sink is located to the west of the hydraulic fracture, indicating that another natural fracture that is not explicitly included in our fracture network model was likely to intersect the west boundary of the hydraulic fracture.

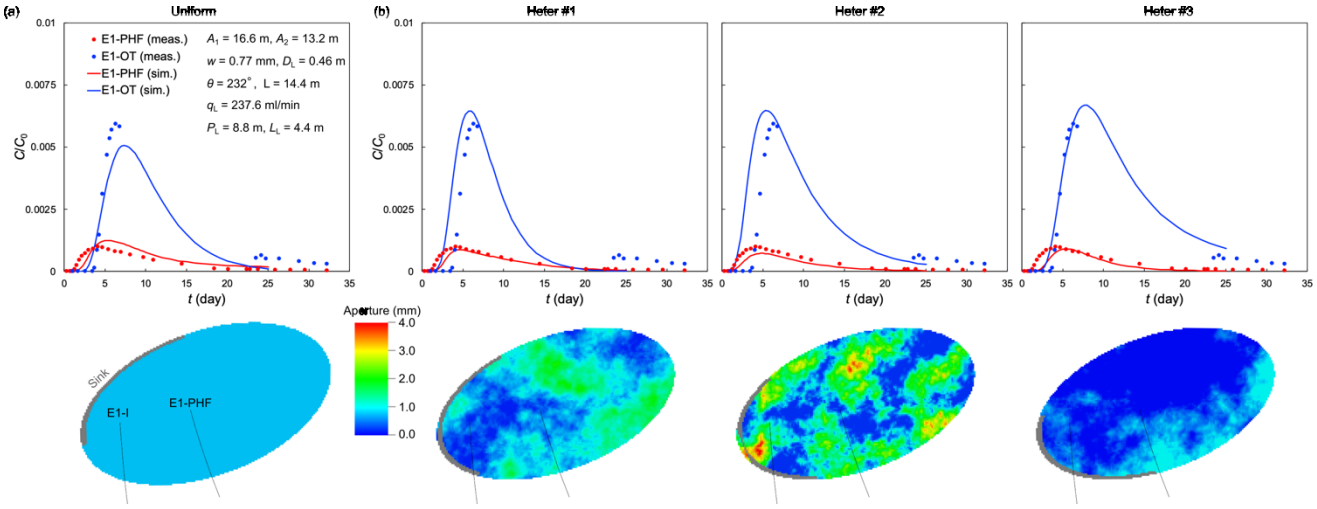

Figure 4: Comparison of tracer BTCs and the corresponding aperture fields from stochastic modeling. (a) Results of the realization that yield the best fit of the tracer BTCs under uniform aperture scenario. (b) Results of three realizations that match the tracer BTCs under heterogeneous aperture scenario.

4.2 Thermal responses analysis

The obtained aperture field and sink location/length in Fig. 4 are then incorporated in the 3D thermal model to simulate the chilled-water circulation test. We mark the four cases as Uniform, Heter #1, Heter #2 and Heter #3 respectively as shown in Fig. 4, and the corresponding temperature responses at E1-PHF are shown in Fig. 5. According to the temperature responses, the thermal breakthrough time is almost the same for the four cases (approximately 22 days after chilled-water injection). The times for 0.5 °C and 1 °C temperature decrease at E1-PHF are also calculated and annotated in Fig. 5(a). In general, a heterogeneous aperture scenario shows a faster thermal decrease than the uniform aperture scenario due to flow channeling (Guo et al., 2016). However, in our thermal model, the flow in the hydraulic fracture is controlled by not only the aperture distribution but also the location of the sink (Fig. 4). Compared to the sink locations for the three heterogeneous aperture realizations, the sink location of the uniform aperture realization is relatively closer to E1-PHF, which inevitably causes preferential water flow towards E1-PHF.

Fig. 5(b) further compares the effects of thermal conduction due to the cooling of E1-I and thermal convection within the hydraulic fracture. The thermal response at E1-PHF due to thermal conduction effect is the same for the four cases. In the first four months of the chilled-water circulation test, the temperature decreases at E1-PHF caused by thermal conduction is similar to that caused by thermal

convection. Afterward, the thermal conduction effect gradually shows more significant impact on the temperature decrease at E1-PHF than the thermal convection effect.

Note that the Joule-Thompson heating effect due to pressure drop at the production well is not considered in the present study. As mentioned by White and Fu (2020), the Joule-Thompson may cause an increase in the temperature at E1-PHF of several degrees. To better interpret the field temperature measurements at the production well and understand the thermal processes in the testbed, we need to incorporate the Joule-Thompson effect in the future simulations.

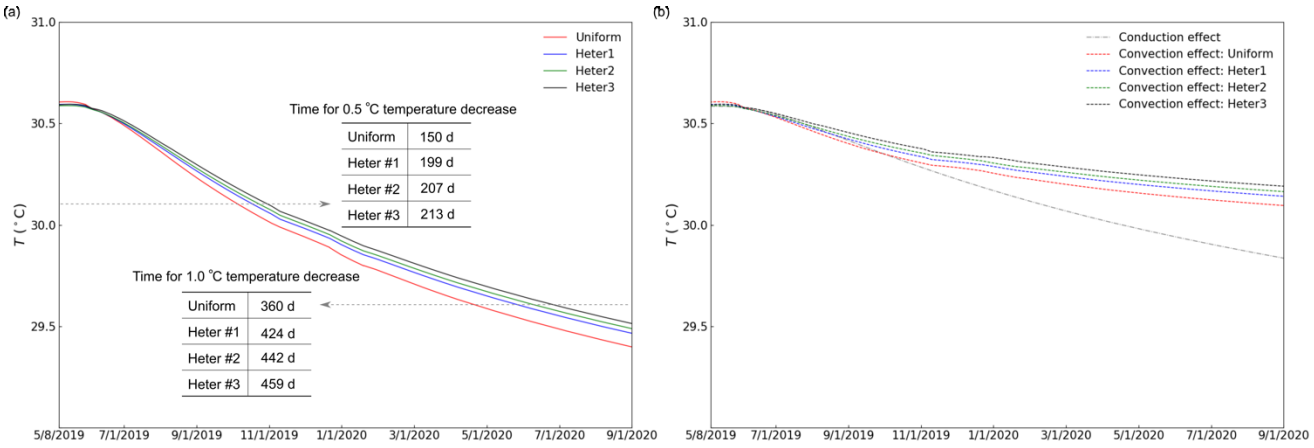

Figure 5: Thermal responses at E1-PHF for the four realizations obtained from tracer modeling. (a) Both the thermal conduction effect due to the cooling of E1-I and the thermal convection effect within the hydraulic fracture are considered. (b) Comparison of the effects of thermal conduction and thermal convection.

5. CONCLUSIONS

The present study analyzed the tracer data at the EGS Collab Experiment 1 through a stochastic tracer modeling approach. Parameters controlling the flow field in the hydraulic fracture, including the aperture distribution and the location and length of a sink on the on the periphery of the hydraulic fracture, are estimated and further used for subsequent thermal modeling to predict thermal responses at the production well.

Both the uniform and heterogeneous aperture scenarios can match the measured tracer BTCs, and four realizations (one from the uniform aperture scenario and three from the heterogeneous aperture scenario) are obtained and used in the following thermal modeling. The predicted thermal breakthrough time is almost the same for the four realizations. However, in the late period of the chilled-water circulation test, the temperature decrease at the production well is faster for the uniform aperture scenario than that for the heterogeneous aperture scenario.

The thermal conduction effect due to the cooling of the injection well shows more significant impact on the thermal response at the production well compared with the thermal convection effect within the hydraulic fracture, especially in the late period of the chilled-water circulation test.

ACKNOWLEDGEMENT

This material was based upon work supported by the U.S. Department of Energy, Office of Energy Efficiency and Renewable Energy (EERE), Office of Technology Development, Geothermal Technologies Office, under Award Number DE-AC52-07NA27344. Publication releases for this manuscript are under LLNL-CONF-803564. The United States Government retains, and the publisher, by accepting the article for publication, acknowledges that the United States Government retains a non-exclusive, paid-up, irrevocable, world-wide license to publish or reproduce the published form of this manuscript, or allow others to do so, for United States Government purposes. The research supporting this work took place in whole or in part at the Sanford Underground Research Facility in Lead, South Dakota. The assistance of the Sanford Underground Research Facility and its personnel in providing physical access and general logistical and technical support is acknowledged.

REFERENCES

Ayling, B.F., Hogarth, R.A., Rose, P.E.: Tracer testing at the Habanero EGS site, central Australia, *Geothermics*, **63**, (2016), 15-26.

Brown, D.W., Duchane, D.V., Heiken, G., Hriscu, V.T.: Mining the earth's heat: Hot dry rock geothermal energy, Springer-Verlag (2012).

Fu, P., Hao, Y., Walsh, S.D.C., Carrigan, C.R.: Thermal drawdown-induced flow channeling in fractured geothermal reservoirs, *Rock Mechanics and Rock Engineering*, **49**, (2016), 1001-1024.

Fu, P., White, M.D., Morris, J.P., Kneafsey, T.J., EGS Collab: Predicting hydraulic fracture trajectory under the influence of a mine drift in EGS Collab Experiment 1, 43rd Stanford Geothermal Workshop, Stanford University, Stanford, CA (2018).

Guo, B., Fu, P.C., Hao, Y., Peters, C.A., Carrigan, C.R.: Thermal drawdown-induced flow channeling in a single fracture in EGS, *Geothermics*, **61**, (2016), 46-62.

Hawkins, A.J., Becker, M.W., Tester, J.W.: Inert and adsorptive tracer tests for field measurement of flow-wetted surface area, *Water Resources Research*, **54**, (2018), 5341-5358.

Kneafsey, T.J., Blankenship, D., Knox, H.A., Johnson, T.C., Ajo-Franklin, J.B., Schwering, P.C., Dobson, P.F., Morris, J.P., White, M.D., Podgorney, R., Roggenthen, W., Doe, T., EGS Collab Team: EGS Collab project: Status and progress, 44th Stanford Geothermal Workshop, Stanford University, Stanford, CA (2019).

Radilla, G., Sausse, J., Sanjuan, B., Fourar, M.: Interpreting tracer tests in the enhanced geothermal system (EGS) of Soultz-sous-Forêts using the equivalent stratified medium approach, *Geothermics*, **44**, (2012), 43-51.

Rodrigues N.E.V., Robinson, B.A., Counce, D.A.: Tracer experiment results during the long-term flow test of the Fenton Hill reservoir, 18th Workshop on Geothermal Reservoir Engineering, Stanford University, Stanford, CA (1993).

Shook, G.M.: Predicting thermal breakthrough in heterogeneous media from tracer tests, *Geothermics*, **30**, (2001), 573-589.

Vogt, C., Kosack, C., Marquart, G.: Stochastic inversion of the tracer experiment of the enhanced geothermal system demonstration reservoir in Soultz-sous-Forêts — Revealing pathways and estimating permeability distribution, *Geothermics*, **42**, (2012), 1-12.

White, M.D., Fu, P.C., Ghassemi, A., Huang, H., Rutqvist, J., Johnston, B., EGS Collab: Numerical simulation applications in the design of EGS Collab Experiment 1, 43rd Stanford Geothermal Workshop, Stanford University, Stanford, CA (2018).

White, M.D., Johnson, T.C., Fu, P.C., Wu, H., Ghassemi, A., Lu, J.R., Huang, H., Neupane, H., Oldenburg, C., Doughty, C., Johnson, B., Winterfeld, P., Pollyea, R., Jayne, R., Hawkins, A., Zhang, Y.R., EGS Collab Team: The necessity for iteration in the application of numerical simulation to EGS: Examples from the EGS Collab test bed 1, 44th Stanford Geothermal Workshop, Stanford University, Stanford, CA (2019).

White, M.D., Fu, P.: Application of an embedded fracture and borehole modeling approach to the understanding of EGS Collab Experiment 1, 45th Stanford Geothermal Workshop, Stanford University, Stanford, CA (2020).

Wu, H., Fu, P., Morris, J.P., Mattson, E.D., Hawkins, A.J., Zhang, Y., Settgast, R.R., Ryerson, F.J., EGS Collab: Characterizing fracture flow in EGS Collab experiment based on stochastic modeling of tracer recovery, 44th Stanford Geothermal Workshop, Stanford University, Stanford, CA (2019).

Wu, X., Pope, G.A., Shook, G.M., Srinivasan, S.: Prediction of enthalpy production from fractured geothermal reservoir using partitioning tracers, *International Journal of Heat and Mass Transfer*, **51**, (2008), 1453-1466.